Characterisation of Atmospheric Turbulence with Space-Geodetic Observation Techniques

Markus Vennebusch[1], Steffen Schön[1] and Axel Nothnagel[2]

[1]Institut für Erdmessung, Leibniz Universität Hannover, Germany
[2]Institut für Geodäsie und Geoinformation, Universität Bonn, Germany

Introduction

For more than 25 years, space-geodetic observation techniques such as Very Long Baseline Interferometry (VLBI) and Global Navigation Satellite Systems (GNSS) have been used to determine precise station coordinates, Earth orientation parameters and other geophysical parameters. Both techniques use microwaves in the X/S- and L-band of the electromagnetic spectrum, respectively. Thus, these observations are affected by atmospheric refraction (propagation delay and ray bending), scintillation, and attenuation. Both, VLBI and GNSS, are sensitive to long-periodic (e.g, diurnal) variations of atmospheric effects and also to high-frequency refractivity variations (e.g., short-periodic water vapor variations due to atmospheric turbulence). These variations generate phase fluctuations which, in geodesy, are usually treated as error sources. However, considering these fluctuations as signal, both microwave techniques can be used to probe the integral effect of atmospheric turbulence within the propagation medium. To exploit this, a sensor network is planned at the Geodetic Observatory at Wettzell in the Bavarian Forest in Germany using existing VLBI telescopes and augmenting a local GPS network. Observations with this sensor network enable analyses of both temporal and spatial characteristics of turbulence processes within the atmospheric boundary layer.

Very Long Baseline Interferometry (VLBI)

Since the 1970ies signals from extra-galactic radio sources are used for geodetic purposes in order to determine precise station coordinates, Earth orientation parameters and atmospheric properties (e.g., ionospheric and/or tropospheric signal delays). Noise-like radio signals from the X- and S-band are being received by large radio telescopes, recorded on disks and finally correlated on especially designed 'correlators' (Fig. 1 right). Correlating radio signals received by two radio telecopes yields the time delay τ between the reception times of the radio signal at the two antennas. In addition, an interference pattern ('fringes', see Fig. 1 left) is generated which provides the interferometer phase φ with sampling rates of up to 1 Hz. While the former observable also contains effects of long-periodic air pressure and humidity variations, the latter observable can be used to analyse high-frequency refractivity (mainly water vapor) variations and thus (temporal) turbulence effects. A network of several radio telescopes additionally enables investigations of spatial turbulence effects.

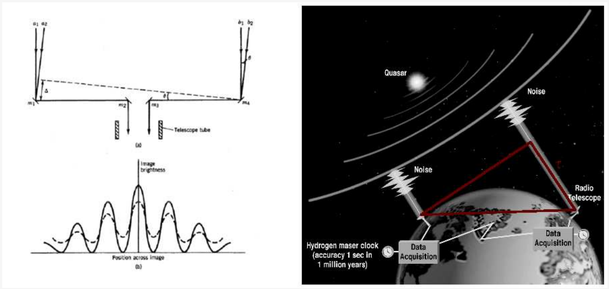

Fig. 1: Basic principle of Very Long Baseline Interferometry (Thompson et al. (2004) and IVS website).

VLBI	GNSS
Interferometer (fringe) phase	In-phase and quad-phase signal component
	Carrier phase observations (residuals)
(Zenith) tropospheric signal delay	(Zenith) tropospheric signal delay

Tab. 1: Space-geodetic observables affected by atmospheric turbulence.

Global Navigation Satellite Systems (GNSS)

Global Navigation Satellite Systems such as the U.S. Global Positioning System (GPS) are based on the use of artificial satellites that emit (phase stable) modulated carrier waves in the L-band. On their way through the atmospheric boundary layer the signals traverse turbulent irregularities which set an irreducible threshold for the accuracy attainable with GNSS. After reception, the GNSS receiver tracks the carrier wave of every visible satellite and thus enables continuous turbulence investigations within the entire elevation range of a satellite.
As with VLBI, the integral effect of atmospheric turbulence along the signal path can be observed. Empirical experiments yielded the following estimate for the integrated profile of the refractive-index structure constant C_n^2 (Wheelon, 2001):

$$\int_0^\infty C_n^2(h)\, dh = 10^{-8}\ [m^{\frac{1}{3}}] \tag{1}$$

Effects of atmospheric turbulence on space-geodetic observations

A model of the impact of atmospheric turbulence on electromagnetic phase observations can be developed by using the geometrical optics approximation and by integrating refractivity variations along the line-of-sight from the receiver to the satellite/radio source (Fig. 2; Wheelon, 2001). A covariance model for GNSS phase observations on the basis of the von Karman turbulence power spectrum has been developed by Schön/Brunner (2008) and reads:

$$\langle \varphi_A^i(t_A), \varphi_B^j(t_B) \rangle = \frac{0.31\ \kappa_0^{-\frac{2}{3}}}{\sin\varepsilon_A^i \sin\varepsilon_B^j} C_n^2 \times \int_0^H \int_0^H (\kappa_0 d)^{\frac{1}{3}} K_{-\frac{1}{3}}(\kappa_0 d)\ dz_1\ dz_2. \tag{2}$$

Equation (2) has to be solved numerically and can be used as a stochastic model for GNSS data analysis and for the simulation of tropospheric signal path variations (Vennebusch et al., 2010; for parameter descriptions, see Tab. 2).

Variable:	Description:	Variable:	Description:
$\varphi_A^i(t_A)$	Phase observation at station A to satellite i (at time t_A)	$\varphi_B^j(t_B)$	Phase observation at station B to satellite j (at time t_B)
C_n^2	Structure constant of refractivity	ε_A^i	Elevation of satellite i at station A
$\kappa_0 = 2\pi/L_0$	Turbulence wavenumber to corresponding outer scale length L_0	d	Separation distance between actual integration points
$k = 2\pi/\lambda$	Electromagnetic wavenumber of signal wavelength λ	H	Height of wet troposphere
K	modified Bessel function of 2. kind		

Tab. 2: Parameter descriptions for Eq. (2).

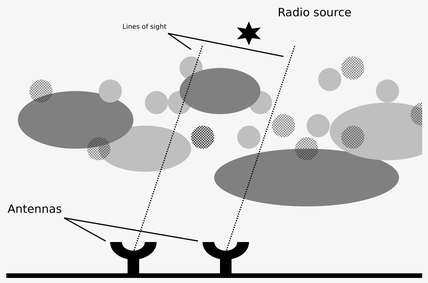

Fig. 2: (Interferometer) phase fluctuations caused by turbulent water vapor irregularities.

Results from dedicated GPS networks

Using specially designed GPS networks, both temporal and spatial characteristics of atmospheric turbulence can be studied. As an example, Fig. 3 shows the so-called Seewinkel network of six equally equipped L1/L2-GPS-receivers located along a 16 km straight line. Both pseudorange and carrier phase data has been recorded for approximately eight hours with a sampling interval of 30 s. Using the 'Precise Point Positioning' technique, this data has been processed to derive high-frequency zenith tropospheric path delays T. These time series were used to generate temporal structure functions via

$$D_T(\tau) = \langle [T(t+\tau) - T(t)]^2 \rangle, \tag{3}$$

with $\langle\ \rangle$ denoting an ensemble average and τ indicating the time lag between two values of T. Replacing τ by sensor distances ρ yields spatial structure functions.
The temporal characteristics (Fig. 4) shows a power-law behaviour with a smooth transition between exponents of 5/3, 2/3, and finally 0. The spatial behaviour (Fig. 5) follows a 2/3-power law behaviour, i.e., the station separation is large compared to the effective tropospheric height so that the turbulence process can be considered as two-dimensional.

Fig. 3: Seewinkel network geometry.

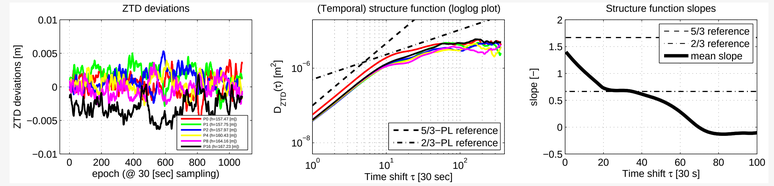

Fig. 4: Temporal characteristics of GPS-derived tropospheric signal delays.

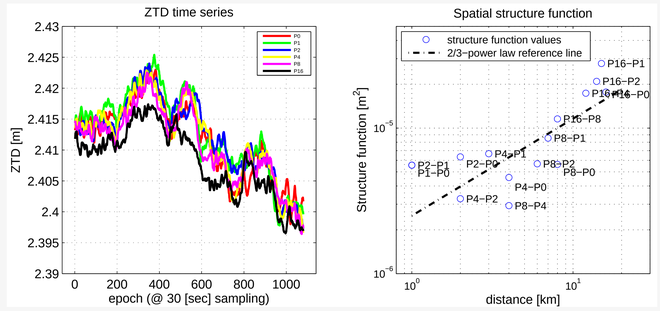

Fig. 5: Spatial characteristics of GPS-derived tropospheric signal delays.

References & Acknowledgements

International VLBI Service for Geodesy & Astrometry: http://ivscc.gsfc.nasa.gov
Schön S, Brunner FK: Atmospheric turbulence theory applied to GPS carrier-phase data, J Geod 82(1): 47-57, 2008.
Thompson AR, Moran JM, Swenson GW: Interferometry and Synthesis in Radio Astronomy, Wiley, 2004.
Vennebusch M, Schön S, Weinbach U: Temporal and spatial stochastic behaviour of high-frequency slant tropospheric delays from simulations and real GPS data, Advances in Space Research, Special Issue: GNSS Remote Sensing, Elsevier, 2010.
Wheelon AD: Electromagnetic scintillation-I. Geometrical optics, Cambridge University Press, Cambridge, 2001.

The authors thank the German Research Foundation (Deutsche Forschungsgemeinschaft) for its financial support (SCHO 1314/1-1) and Fritz K. Brunner (IGMS, TU Graz) for the permission to use the Seewinkel data in this study.

Institut fur Erdmessung
Schneiderberg 50
D-30167 Hannover

EGU 2011
3 - 8 April 2011

Markus Vennebusch
Steffen Schön, Axel Nothnagel
www.ife.uni-hannover.de
{vennebusch, schoen}@ife.uni-hannover.de, nothnagel@uni-bonn.de